Available online at www.sciencedirect.com

ScienceDirect

Acta Materialia 92 (2015) 197–208

Acta MATERIALIA

www.elsevier.com/locate/actamat

Phase-field model coupling cracks and dislocations at finite strain

Antoine Ruffini* and Alphonse Finel[1]

Laboratoire d'Étude des Microstructures, CNRS-ONERA, B.P. 72, F92322 Châtillon Cedex, France

Received 19 February 2015; accepted 3 April 2015
Available online 22 April 2015

Abstract—A new 3D continuum model is developed to simultaneously describe cracks and dislocations in materials undergoing finite strain deformations. Significant advances are made to account for fracturing in a cubic symmetrical system and to correctly model the microscopic dislocation properties into a Time-Dependent Ginzburg–Landau formalism. In addition, the interaction between dislocations and free borders (crack lips, surfaces. . .) is naturally described. As an example, the model is used to investigate the effects of plasticity on the delamination and buckling of thin films deposited on substrates. It may also be helpful in any other situation where cracks and dislocations take place and in which finite strain effects must be considered.

Keywords: Cracks; Dislocations; Finite strains; Phase-field; Buckling

1. Introduction

Generally, alloys and metals used in industry are materials which exhibit strong heterogeneities since they are composed of a microstructure that couples a wide variety of multiscale physical phenomena. In some alloys for example, the formation of precipitates is observed at a micrometer scale while, at a lower scale, they appear as obstacles to the motion of dislocations manifesting as a drastic change of the macroscopic mechanical properties [1]. Interfaces between two phases also constitute preferential sites for the damage to occur, especially because they localize stress concentrations that often result in the spontaneous formation of microcracks and dislocations [2]. Similar phenomena are also identified in coating devices where microscopic mechanisms induce delamination and buckling of structures standing themselves at a micrometer scale [3,4].

Numerically, in strategies which consist of describing these coupled phenomena, simulations operating at the discrete atomic scale seem to be the most relevant. However, these methods are often computationally expensive and, despite their constant improvements, it seems that they never allow the investigation of macroscopic objects at realistic space and time scales.

Therefore, alternative descriptions have been introduced, taking advantage of numerical progress and the recent development of new methods, among which is the phase-field. Within this framework, an element of the microstructure is described as a region of space with specific physical properties wherein a field subject to certain dynamics reflects its presence or not at a given point of the material. At the beginning of the last decade, these methods, already used to investigate phase transformations [5], have been extended to describe crystal defects such as cracks [6–9] and dislocations [10–15].

Today, these methods are used to solve problems involving cracks and dislocations taken independently, often coupled with other kinds of fields related to other physical mechanisms [16,17]. However, to our knowledge, none of these studies explicitly couple cracks and dislocations together. This challenge is nevertheless essential in material science since the macroscopic damage of materials is most likely the result of the coupling between such fundamental mechanisms [18]. Moreover, the finite strain effects are usually not considered in the description of that kind of phenomena, except for dislocations in Ref. [19], which is nevertheless crucial in some cases [20].

In this paper, we propose a continuum model describing quasi-static microcracks and dynamic dislocations within an elastic framework formulated at finite strain. The coupling between these objects is achieved in a physical way, within a numerical description that allows the consideration of heterogeneities and free-surfaces. As an example, the model is used in the buckling context which requires one such description.

The paper is organized in two sections. In the first, the finite strain continuum model for fracturing is exposed and illustrated with simple examples. In the second, the model is extended to account for plasticity in a Time-Dependant Ginzburg–Landau formalism also formulated

* Corresponding author; e-mail addresses: antoine.ruffini@onera.fr; alphonse.finel@onera.fr

[1] Principal corresponding author.

http://dx.doi.org/10.1016/j.actamat.2015.04.013
1359-6462/

at finite strain. The coupling between cracks and dislocations is finally achieved and subsequently used in the buckling context.

2. Continuum model for fracturing

2.1. Elastic background

The model reproduces the behavior of cubic symmetrical materials within the linear elasticity theory. The total free elastic energy $\mathcal{F}_{el}$ is then defined by the following functional [21]:

$$\mathcal{F}_{el} = \int_V f_{el}(\mathbf{r})\mathrm{d}V, \tag{1}$$

where V is the volume of the material and f_{el} is the free elastic energy density defined at position $\mathbf{r}$ by:

$$\begin{aligned} f_{el} = {} & \frac{K}{2}(\varepsilon_{11}+\varepsilon_{22}+\varepsilon_{33})^2 \\ & + \frac{C'}{3}\left[(\varepsilon_{11}-\varepsilon_{22})^2+(\varepsilon_{11}-\varepsilon_{33})^2+(\varepsilon_{22}-\varepsilon_{33})^2\right] \\ & + \frac{\mu}{2}\left[(2\varepsilon_{12})^2+(2\varepsilon_{13})^2+(2\varepsilon_{23})^2\right]. \end{aligned} \tag{2}$$

In Eq. (2), ε_{ij} denotes the strain tensor components and K, C' and μ are the bulk modulus, the shear modulus and the second Lamé coefficient, respectively. These moduli are position-dependent to account for different materials within a single system. It is worth noting that C' and μ are equal to each other in the isotropic case.

In a fixed Cartesian frame $(X_i)_{i=1,3}$, finite effects are taken into account through the Green–Lagrange strain tensor whose components are:

$$\varepsilon_{ij}(\mathbf{r}) = \frac{1}{2}\left(\beta_{ij}(\mathbf{r}) + \beta_{ji}(\mathbf{r}) + \sum_{k=1}^{3}\beta_{ki}(\mathbf{r})\beta_{kj}(\mathbf{r})\right), \tag{3}$$

where β_{ij} are the displacement-gradients:

$$\beta_{ij}(\mathbf{r}) = \frac{\partial u_i(\mathbf{r})}{\partial X_j}, \tag{4}$$

in which u_i are the displacement vector components. It is worth mentioning that the use of linear elasticity with finite strains is only justified in situations where large rotations are involved and where physical phenomena (cracks, dislocations…) prevent large stretching to occur.

The mechanical equilibrium is obtained with a dissipative dynamic in which the temporal variation of the displacements u_i is proportional to the functional derivative of the free elastic energy $\mathcal{F}_{el}$ with respect to u_i (i.e. the mechanical force):

$$\frac{\partial u_i(\mathbf{r},t)}{\partial t} = -M\frac{\delta \mathcal{F}_{el}}{\delta u_i(\mathbf{r},t)}. \tag{5}$$

where M is a dissipative coefficient for the elastic field and $\mathcal{F}_{el}$ is the functional of the free elastic energy given Eq. (1). Thus, inertial effects are not involved in the present model.

2.2. Numerical implementation

Numerically, the continuum fields are discretized on a cubic grid whose nodes are places where displacements u_i are expressed and cubic volumes are elementary "voxels" where strains ε_{ij} (or equivalently the elastic energy) are calculated. Thus, any material is seen as a juxtaposition of elementary voxels that contain an elastic energy contribution.

In Fig. 1, one of these voxels is displayed to highlight in more detail how the elastic energy is calculated. Each summit is related to three length elements $\mathrm{d}X_j$ labeled from 1 to 4 in the first direction of space, from 5 to 8 in the second and from 9 to 12 in the third. The eight summits of the voxel are nodes localized in their current position with coordinates x_i, indexed using the alphanumerical notation $a(+1), b(+1)$ and $c(+1)$. The displacement-gradients β_{ij} defined in Eq. (4) are calculated by using a finite difference scheme where each component is identified to a length change along i of an element $\mathrm{d}X_j$. For example, if we focus on the first summit with elements $\mathrm{d}X_1(1)$, $\mathrm{d}X_2(5)$ and $\mathrm{d}X_3(9)$, the following identification is obtained:

$$\beta_{i1} \equiv \frac{x_i(a+1,b,c)-x_i(a,b,c)}{\mathrm{d}X_1(1)}, \tag{6}$$

$$\beta_{i2} \equiv \frac{x_i(a,b+1,c)-x_i(a,b,c)}{\mathrm{d}X_2(5)}, \tag{7}$$

$$\beta_{i3} \equiv \frac{x_i(a,b,c+1)-x_i(a,b,c)}{\mathrm{d}X_3(9)}, \tag{8}$$

which explicitly gives the displacement-gradients tensor for this summit. This tensor allows us to determine the Green–Lagrange strain tensor (see Eq. (3)) from which the elastic energy is calculated (see Eq. (2)). An elastic energy is thus established for each summit of the voxel that represents an eighth of its total elastic energy f_{vox}. By fixing elements $\mathrm{d}X_j$ at the same length d, the elastic energy density given by Eq. (2) is finally identified as $f_{el} = f_{vox}/d^3$. It is worth mentioning that d is a grid spacing which does not (yet) have physical meaning. This length must simply be greater than the local radius curvature to prevent any numerical artifacts.

To obtain the mechanical equilibrium, each node of the grid is assumed to be in the environment of its closest eight voxels. The total elastic energy at the position of a node f_{node} is thus the sum of the eight elastic contributions f_{el} of these voxels. By conserving these notations, Eq. (5) finally rewrites as:

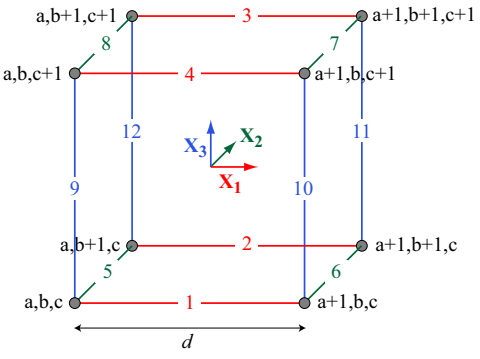

Fig. 1. Schematic of a voxel whose summits are nodes represented by a gray disk and edges are length elements $\mathrm{d}X_j$. The grid spacing (the edges of the cube) has been fixed at d.